This is the peer reviewed version of the following article: Ettorre V., et al. Carbon 2016, 103, 291-298, which has been published in final form at https://www.sciencedirect.com/science/article/pii/S0008622316301993?via%3Dihub.

This article may be used for non-commercial purposes in accordance with Elsevier Terms and Conditions for Use of Self-Archived Versions.

In vitro and in vivo characterization of graphene oxide coated porcine bone granules

Valeria Ettorre,[1,‡] Patrizia De Marco,[1‡] Susi Zara,[1,‡] Vittoria Perrotti,[2,‡] Antonio Scarano,[2] Antonello Di Crescenzo,[1] Morena Petrini,[2] Caroline Hadad,[3] Domenico Bosco,[4] Barbara Zavan,[5] Luca Valbonetti,[6] Giuseppe Spoto,[2], Giovanna Iezzi,[2] Adriano Piattelli,[2] Amelia Cataldi,[1] Antonella Fontana[1,*]

[1]*Department of Pharmacy, University "G. d'Annunzio", Via dei Vestini 31, 66100 Chieti, Italy*

[2]*Department of Medical, Oral and Biotechnological Sciences, University "G. d'Annunzio", Via dei Vestini 31, 66100 Chieti, Italy*

[3]*Center of Excellence for Nanostructured Materials (CENMAT), INSTM, Department of Chemical and Pharmaceutical Sciences, University of Trieste, Piazzale Europa 1, 34127 Trieste, Italy*

[4]*Molecular Genetics Institute, CNR Unit of Chieti, 66100, Italy*

[5]*Department of Biomedical Sciences, University of Padova, Via Ugo Bassi, 58/B 35121 Padova, Italy*

[6]*Department of Comparative Biomedical Science, University of Teramo, Piazza Aldo Moro 45, 64100 Teramo, Italy*

‡These authors contributed equally.

* Corresponding author. E-mail: antonella.fontana@unich.it (Antonella Fontana). Phone number: +39 08713554790; Fax number: +39 08713554912

ABSTRACT. Graphene oxide (GO) demonstrated to improve the wound healing properties of materials intended for bone replacement. The main objective of this study was the setting up of a simple and effective procedure for the production of GO-coated porcine bone (PB) granules and the characterization of the obtained material in order to improve its properties by exploiting chemical, physical, biological and mechanical features that the GO coating could confer to pre-formed PB granules. The obtained coating was homogeneously distributed on PB granule surface and demonstrated to confer PB an increased resistance to fracture load. Biological analyses evidenced no toxic effects of GO-coated PB samples on primary human gingival fibroblasts, and no inflammatory response around the grafted particles when implanted in vivo on a sheep model although GO-coated PB samples did not appear to improve new bone formation efficacy compared with the control within the investigated time. A small loss of GO was however detected, indicating the opportunity to investigate less GO concentrated samples. In conclusion, this study presents a novel and low cost approach to the development of functionalized biomimetic hybrid materials which can be applied to other bone substitute materials in order to improve their performances.

Key words: biocompatibility, graphene oxide, porcine bone

1. Introduction

Currently, an extraordinary interest is devoted to explore the potential of graphene for possible applications in biomedical and regenerative engineering. Graphene is a two dimensional allotrope of carbon with only one atom thickness, i.e. a planar sheet of condensed benzene rings. This structure confers graphene an extraordinary high mechanical stiffness [1], an exceptional high thermal [2] and electrical conductivity [3,4], and makes graphene ideal to be used as coating of materials that usually lack these properties. The strongest limitation of graphene practical applications is its poor solubility in both organic solvents and water, and therefore its difficult handling. Indeed, once exfoliated, graphene tends to reaggregate due to weak but extensive non-covalent interactions among its sheets [5]. Researchers have overtaken this drawback by exploiting chemical covalent functionalization [6,7,8]. In particular, oxidation appears to be the easiest and lowest cost functionalization available, enabling the insertion into graphene carbon backbone of a series of differently oxidized functionalities such as hydroxyl, ether and epoxyl groups on their basal plane and carboxyl and carbonyl located mainly at the sheet edges [9] that confer to graphene a hydrophilicity proportional to the degree of oxidation. Graphene oxide (GO) has thus been extensively investigated as an additive for biomedical materials thanking to its capacity to promote the adhesion, proliferation, and differentiation of various cells [10,11].

Nowadays, heterologous materials are included among the most commonly used biomaterials for bone replacement and bone regeneration, and they are considered excellent

bioactive and osteoconductive materials [12]. However, these tissue derived materials, as well as the synthetic hydroxyapatite (HA) counterpart, are brittle and characterized by low fracture toughness and merely osteoconductive properties. These drawbacks could be overcome by using different materials such as alumina, titania and carbon nanotubes (CNT) [13]. We thought to improve pre-formed porcine bone (PB) granules features by using GO. As a matter of fact, despite functionalization alters graphene features [9], GO keeps its extraordinary mechanical stiffness and strength, and hopefully may act as an osteoinductive factor [14].

Actually, a few studies have been published on the use of GO for possible applications in biomedical and regenerative engineering, such as induction of differentiation of mesenchymal stem cells towards osteoblastic lineage [15-17] and formation of *in situ* hydroxyapatite HA via precipitation of calcium phosphate [18-20].

To our best knowledge no studies are available reporting on GO in vivo application for bone regeneration, or on the development of a GO coating for commercially available bone substitute materials. Thus, the main aim of the present study was to set up an easy and inexpensive protocol for the preparation of GO-coated PB granules and to characterize the obtained material through the investigation of the chemical, physical, biological and mechanical features that the GO coating could confer to pre-formed PB granules.

Materials and Methods

2.1 Preparation of graphene oxide

Graphene oxide (GO) was prepared from graphite by using a modified Hummers method [21,22]. A flask containing a mixture of 0.2 g of graphite and 0.1 g of sodium nitrate in 4.6 mL of concentrated sulfuric acid was placed in an ice bath. Then 0.6 g of potassium permanganate was added slowly under continuous stirring. After 2 h, the reaction mixture was transferred in a water bath at 35 °C and stirred for 30 min. 9.2 mL of deionized water were slowly added into the solution (the monitored solution temperature was about 98 °C) and this temperature was ensured by heating for further 45 min. 27.8 mL of deionized water and 2.14 mL of 30% hydrogen peroxide were poured in the mixture to stop the reaction. The obtained light brown mixture was filtered through a sintered-glass filter (pore size 15-40 µm) and rinsed three times with 5% HCl and then with water. The solid was dried at 60°C for 12h. The obtained graphite oxide was redispersed in water, ultrasonicated for 45 min and centrifuged for 15 min at 9000 rpm. Rotary evaporation at 40 °C of the corresponding supernatant allowed to obtain exfoliated GO.

2.2 Preparation of GO-coated PB granules

25 mL of a homogeneous dispersion of GO in water at various concentrations (50, 75, 100 µg/mL), preventively ultrasonicated for 30 min and centrifuged at 5500 rpm for 15 min, were added to 50 mg of PB granules. After 15 min, solvent was evaporated at reduced

pressure and controlled temperature (40 °C) on a rotary evaporator. At the end of the procedure, uniformly coated PB granules were obtained.

2.3 Materials

Synthetic Graphite ~ 200 mesh, 99.9995% powder was purchased from Alfa Aesar. PB granules (APATOS CORTICAL, OSTEOBIOL®) were a gift of Tecnoss dental s.r.l. Pianezza (TO), Italy. All other reagents of analytical grade were used as received. The Dulbecco's modified Eagle's medium DMEM, fetal bovine serum (FBS), antibiotics (penicillin and streptomycin) and fungizone were purchased from Euroclone, Pero, MI, Italy. MTT (3-[4,5-dimethyl-thiazol-2-yl]-2,5-diphenyltetrazolium bromide) and DMSO (dimethylsulfoxide) were purchased from Sigma Aldrich, Saint Louis, MO, USA. Ivermectin (Ivomec ovini) was purchased from Merial Italia, Milano, Italy. Xylazine (Rompum®) was purchased from Bayer. Diazepam (Diazepam® 0,5), ketamine (Ketavet® 100), embutramide (TanaxH) and thiopental (Pentothal Sodium) were purchased from Intervet, Italia. Atropine sulfate was purchased from Fort Dodge. Halothane (Halotane®) was purchased from Merial. The glycolmethacrylate resin was purchased from Technovit 7200 VLC, Kulzer, Wehrheim, Germany.

2.4 Apparatus for chemico-physical characterization of the material

The morphology of GO nanosheets and GO-coated PB granules was evaluated by Scanning Electron Microscopy (JEOL 6360LV SEM microscope - JEOL, Tokyo, Japan) and Transmission Electron Microscopy (TEM, Zeiss Electron microscope 109). Samples for SEM were fixed with 2.5% glutaraldehyde in 0.1 M cacodylate buffer for 1 h before being

processed either with hexamethyldisilazane or at the critical point followed by gold-palladium coating. All SEM micrographs were obtained at 30 kV. GO samples for TEM imaging were prepared by dispersion of materials in water, followed by ultrasonication. A drop of suspension (5 μl) was placed onto carbon coated copper grids, dried in air and loaded into the electron microscope chamber. GO-coated PB granules were directly placed onto carbon coated grids. Raman spectra were recorded on an Invia Renishaw microspectrometer (50 or 100×) by using a laser source at 532 nm (power 5%, 3 or 5 accumulations/measurement). GO was drop-casted onto silicon wafers while PB or GO-enriched PB powder were gently compressed using a glass slide. The Fourier transformed infrared spectrum (FTIR) was measured with a Varian FTS 1000 spectrometer. The UV-Vis absorption spectrum was carried out by using a Varian Cary 100 UV–Vis spectrophotometer. Thermo-gravimetric analyses (TGA) on ca. 5 mg sample were performed under nitrogen by setting a temperature increment of 5 °C/min from 0 to 600 °C; the hybrid samples were grinded in a ceramic mortar. Measurements of average size and ζ-potential values were performed by using a 90Plus/BI-MAS ZetaPlus multiangle particle size analyzer (Brookhaven Instruments Corp.). For optical microscopy measurements the 50 μg/mL GO-coated PB granules were embedded in a glycolmethacrylate resin (Technovit 7200 VLC, Kulzer, Wehrheim, Germany), the specimens were sectioned with a high precision diamond disk at about 150 μm. The samples were stained with acid fuchsin and toluidine blue. Histomorphometry of newly formed bone, marrow spaces and residual biomaterial was carried out using a light microscope (Laborlux S, Leitz, Wetzlar, Germany) connected to a high resolution video camera (3CCD, JVC KY-F55B) and interfaced to a

monitor and PC (Intel Pentium III 1200 MMX). This optical system was associated with a digitizing pad (Matrix Vision GmbH) and a histometry software package with image capturing capabilities (Image-Pro Plus 4.5, Media Cybernetics Inc., Immagini & Computer Snc Milano, Italy).

2.5 Stability of the granules in water

In order to evaluate the stability of the material in aqueous solution, 15 mg of PB and 15 mg GO-coated PB were soaked in 2.4 mL milli-Q water and put it under gentle shaking for 15 h. The aqueous suspensions were left resting for 1 h in order to allow the granules to set down and UV-vis spectra (see Results) of the supernatant were registered.

2.6 Mechanical Investigations

Compression is a fundamental type of test used to characterize biomaterials and many other common materials. Static compression tests apply an escalating compressive load until failure. The mechanical properties of the investigated materials were characterized by using a static materials testing device (Lloyd 30K, Lloyd Instruments Ltd, Segensworth, UK) managed by a dedicated software (Nexigen, Batch Version 4.0 Issue 23, Lloyd Instruments Ltd, Segensworth, UK). Specifically, the compression was performed with a load applied at the granules with a constant crosshead speed of 5 mm/min at 14 granules of pure PB and 14 granules of 50 µg/mL GO-coated PB. The load was applied parallel to biomaterial granules. The fracture load data were automatically recorded using Nexigen software (Nexigen, Batch Version 4.0, Issue 23, Lloyd Instruments Ltd, Segensworth, UK).

Estimation was performed to determine the confidence intervals for the true means of the compression strength values. For the parameter estimation a normal distribution of the

unknown means and their unknown variance was assumed. Hence, a test statistic was computed, which is described by the Student's t-distribution. In this manner the intervals were calculated, which include the true means at a 95% level of confidence.

2.7 Human Gingival Fibroblasts (HGF) culture and MTT [3-(4,5-dimethylthiazol-2-yl)-2,5-diphenyltetrazolium bromide] assay

HGF were obtained from third molar extraction interventions, the donors age ranged from 20 to 40 years, donors were not affected by any systemic conditions, did not take medication and tobacco. HGF, obtained from fragments of healthy gingival tissue were immediately placed in Dulbecco's modified Eagle's medium DMEM, rinsed in phosphate buffered saline solution (PBS), minced into small tissue pieces and cultured in DMEM containing 10% fetal bovine serum (FBS), antibiotics (1% penicillin and streptomycin) and 1% fungizone. The gingival fragments were cultured until HGF appeared. All cells were maintained at 37 °C in a humidified atmosphere of 5% (v/v) CO_2. Cells were processed after 4-8 passages. All the experiments were realized with cells obtained from two different donors.

In order to evaluate the ability of the materials to condition the medium, HGF were seeded in a 96 multiwell plate, dipping in each well three granules of PB and GO-coated PB and cultured in DMEM +10% FBS for 1, 3 and 7 days. After each experimental time an MTT, based on the ability of viable cells to reduce MTT into a colored formazan product, was carried out.

In order to evaluate the effect of a direct contact between cells and granules, HGF were seeded in a 96 multiwell plate on PB and GO-coated PB granules, previously immobilized

in a thin layer of Agar 2%, cultured in DMEM +10% FBS for 1,3 and 7 days, and processed for MTT test.

In order to perform MTT assay, the medium was replaced by a fresh one containing 0.5 mg/mL MTT and probed with cells for 5 h at 37 °C. The plate was incubated in DMSO solution for 30 min at 37 °C to solubilize salts and then read at 570 nm. Values obtained in the absence of cells were considered as background.

2.8 Statistical analysis

Statistical analysis was performed using SPSS software (Statistical Package for Social Science) GraphPad Prism 5 and evaluation with t-test. The results were expressed as means ± SD significant. We considered significant p values <0.05**.**

2.9 Histology

Two Italian Appenninica sheep, aged 2 years old and of 40–50 kg of body weight were selected for this study. One week before surgery the animals were de-wormed with 200 μg/kg of ivermectin intramuscularly (i.m.). The animal protocol, authorized by the National Government agency responsible for animal welfare and protection (n 001/2001), is reported in the Supplementary Data.[†] A total of 4 specimens were retrieved from each animal and immediately stored in 10% buffered formalin. The samples were split in two different groups, which were differently handled: the bone specimens and the soft tissues covering the sites grafted with biomaterials. The bone samples (2 PB and 2 GO-coated PB) were then processed using the Precise 1 Automated System (Assing, Rome, Italy). They were dehydrated in a graded series of ethanol rinses and embedded in a glycolmethacrylate resin.

After polymerization, the specimens were sectioned, along their longitudinal axis, with a high precision diamond disk at about 150 μm and ground down to about 30 μm. Three slides were obtained from each specimen and they were stained with acid fuchsin and toluidine blue and examined with transmitted light Leitz Laborlux microscope (Leitz, Wetzlar, Germany). Histological observations were carried out using a light microscope. The soft tissue specimens above the defects filled with the biomaterials were embedded in paraffin and stained with haematoxylin and eosin. In order to analyze the cellular response to GO-coated PB granules, two investigators analyzed in a masked fashion at least 3 slides for each experiment by light microscopy using 20× as initial magnification. Each slide contained three sections of specimen and 5 fields of 322 μm^2 each were analyzed for each tissue section. Experiments were performed at least three times and values were expressed as the mean ± SD.

3. Results

3.1 Characterization of the GO-coated PB granules

The characterization of GO is reported in the Supplementary Data.† GO-coated PB granules, obtained by coating pre-formed PB granules with GO (Figure 1), were characterized by using FTIR, Raman spectroscopies, optical microscopy, TEM, SEM, and TGA.

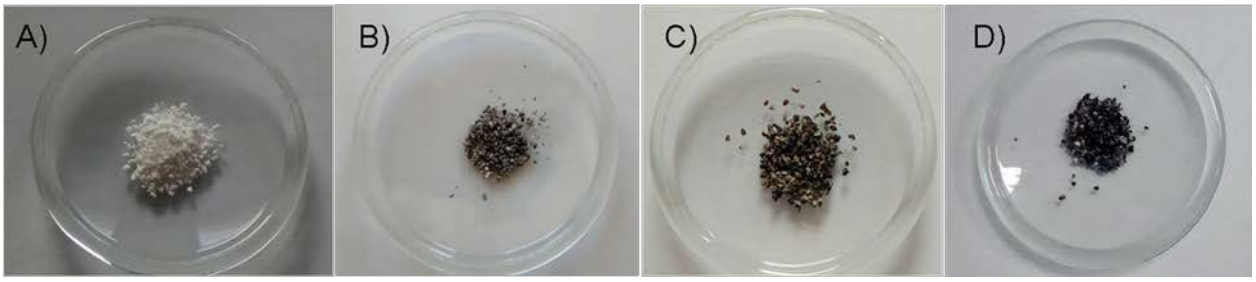

Figure 1. Digital photos of (A) PB granules and GO-coated PB granules obtained by using different GO concentrations (B) 50 μg/mL, (C) 75 μg/mL and (D) 100 μg/mL, respectively.

The FTIR spectra of PB showed characteristic bands of hydroxyapatite, the prevailing constituent of porcine bone tissue (Figure S4)†. The stretching band at around 1036 cm^{-1} was due to phosphate group, that at 874 cm^{-1} was due to carbonate, bands at 565 and 604 cm^{-1} were due to P-O bending of phosphate group. The stretching band of O-H group was around 3430 cm^{-1} whilst the bending band was around 1640 cm^{-1} [18,20,23,24]. Unlikely, this technique is not sensitive enough to allow the recognition of the low percentage of GO used to coat PB granules.

Raman spectra were performed on PB granules and GO-coated PB granules (Figure 2). The spectra of PB were the typical Raman spectra of bone tissue [25] and peaks were easily assignable to mineral and organic phases. In the GO-coated PB granules both PB and GO were well represented.

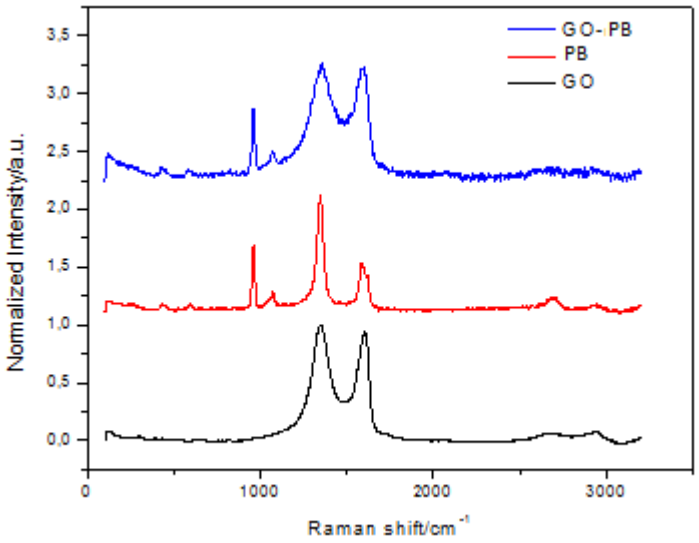

Figure 2. Raman spectra of PB granules (red line), of 50 µg/mL GO-coated PB (blue line), and GO (black line). All spectra were recorded at 532 nm wavelength.

3.2 Microscopy measurements

The observations performed on *in vitro* samples by optical microscope revealed that GO coating layer was relatively well distributed on the granule surface and it was relatively thick (Figure 3A and 3B) compared to the amount of GO used for the coating (see discussion).

TEM image of typical GO-coated PB granules (Figure 3D) clearly showed that few layered GO coated the granules of PB, confirming optical microscopy evidences. Analogously,

GO-coated PB SEM micrographs (Figure 3F) highlighted a relatively smoothness of the surface when GO was added to PB, although this analysis did not allow to further characterize the GO coating.

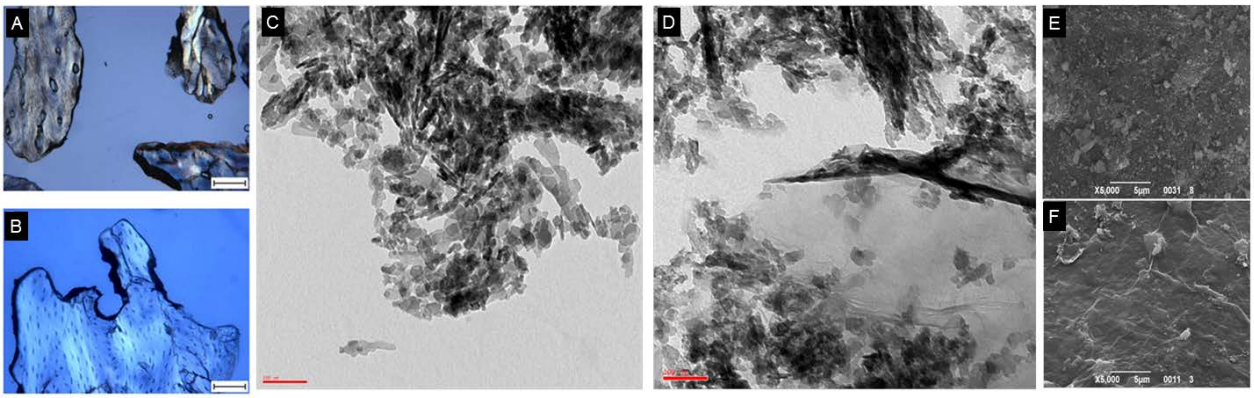

Figure 3 Light microscopy images showing 50 µg/mL GO-coated PB samples (**A** and **B**). Transmission electron microscopy micrographs of PB (**C**) and of the 50 µg/mL GO-coated PB (**D**). Scanning electron microscopy micrographs of commercial PB (**E**) and 50 µg/mL GO-coated PB (**F**). Scale bar is 200 µm; 100 µm in B, 5 µm in E and F, 100 nm in C and D.

3.3 Stability of the granules in water

UV-vis spectra of aqueous supernatant from gentle shaking for 15 h in milli-Q water non-coated (Figure 4A, grey line) and GO-coated PB granules (black line) revealed a higher absorbance at 300 nm (due prevailingly to the presence of hydroxyapatite) for the former aqueous solution indicative of the fact that non-coated granules solubilize in water more calcium phosphate and collagen than the GO-coated PB granules. This evidence is in agreement with the hypothesized leak of calcium as the cause of the thickness of the GO

coating observed with optical microscopy (Figure 3A and 3B). The flat and featureless absorption in the region 350-800 nm [26,27] is indicative of a slight leakage of GO from the GO-coated granules and the absorbance at 660 nm was taken as an indication of GO leakage. From the absorptivity coefficient calculated at 660 nm, i.e. 1.4 mL mg^{-1} cm^{-1}, a release of 0.15% of GO could be determined in the GO-coated PB sample after 15 h. The inset of Figure 4A showed the stability of the granules over time. It is important to underline that at 24 h, the supernatant aqueous solution lost its limpidity and became turbid revealing a progressive increase of absorbance at both monitored wavelengths (i.e. 300 and 660 nm) at least for the first 4 days, then a plateau was reached. Despite it is not possible to quantify the leakage of GO at times longer than 15 h because the scattering of collagen and calcium phosphate overrided the absorbance of GO, the stability data evidenced, as well as the spectrum recorded after 15 h, a higher and easier dissolution of non-coated PB granules with respect to GO-coated PB granules. The leakage of hydroxyapatite and GO from the coated samples was confirmed as well by TEM measurements of a concentrated sample of the same supernatant. Hydroxyapatite appeared in this case as powder homogenously distributed onto GO sheet (Figure 4B).

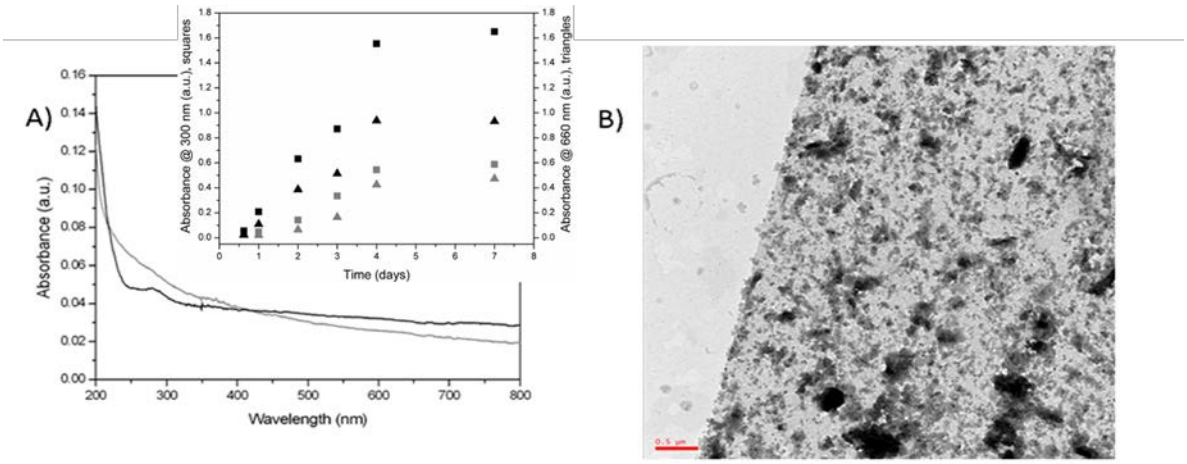

Figure 4. A) UV-vis spectrum of aqueous supernatant from 15 h gentle shaking in milli-Q water of PB granules (grey line) and 50 μg/mL GO-coated PB (black line) granules. Inset: Stability of PB granules (grey symbols) and 50 μg/mL GO-coated PB granules (black symbols) over time, squares refers to absorbance at 300 nm, triangles to absorbance at 660 nm. B) TEM micrographs obtained on supernatants of GO/PB sample. The samples were prepared by concentrating the relevant supernatants on the grid. Scale bar in B) is 0.5 μm.

3.4 Quantification of GO coating

Thermogravimetric analysis (TGA) was used to measure the amount of GO covering the PB granules (Figure 5) by analyzing the weight loss percentage of samples heated at increasing temperatures. During the heating process PB granules and GO-coated PB composite showed a slow and weak weight loss behavior due to their high thermal stability between 0 to 650 °C. On the other hand, GO showed an initial weight loss due to the evaporation of water molecules on its surface and a subsequent weight loss, around 200 °C, ascribed to decomposition of the labile oxygenate functional groups on the GO surface

[24,28]. From the plot, and calculating the percentage of weight loss in the 150-250 °C interval, the GO coating represented 1.58% of PB granules (Figure 5).

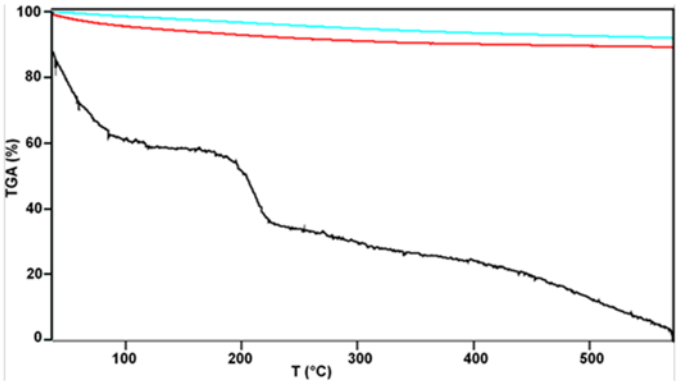

Figure 5. Thermogravimetric analysis of GO (black line), PB granules (blue line) and 50 µg/mL GO-coated PB (red line).

3.5 Mechanical characterization

PB and GO coated PB granules showed a fracture resistance of 4.0±1.0 and 5.5±1.0 N, respectively. A comparative analysis of fracture resistance values between PB group and GO coated PB group shows high statistical significance (P = 0.0019) which was determined by using t-test.

The GO-coating on PB granules led to a composite scaffold with 35% increased resistance. Table S1[†] shows compressive stress values of pure PB granules and GO-coated porcine bone granules and statistical comparison between the two groups.

3.6 Evaluation of biocompatibility

A preliminary evaluation of GO-coated PB granules biocompatibility was realized seeding HGF on the polystyrene surface of the multiwell plate and dipping GO-coated PB granules in the culture medium thus realizing a medium conditioning. No differences of HGF viability were found between PB and GO-coated PB granules by means of MTT. This initial evaluation indicated that GO-coated PB granules did not condition the medium and let us to hypothesize that they did not leak toxic species in the liquid in which they were immersed under the experimental conditions adopted.

Then, to obtain a direct contact between HGF and granules, the model was improved by immobilizing granules in a thin layer of Agar and seeding the cells on the granules. After 1, 3 and 7 days of culture an MTT assay was performed to evaluate HGF viability and, as a consequence, GO-coated PB biocompatibility. Results showed at day 1 no statistically significant differences in MTT measurements between PB and PB granules coated with different concentration of GO (i.e. 50 μg/mL GO for GO50/PB and 100 μg/mL GO for GO100/PB, respectively). After 3 days of culture HGF viability slightly increased in the presence of GO100/PB with respect to PB. After 7 days of culture MTT assay evidenced a slight HGF viability decrease in the GO50/PB sample, with respect to PB (Figure 6). The above mentioned changes with respect to those observed for non-coated granules were not statistically significant. These preliminary evidences clearly suggested that GO coating, either performed at 50 μg/mL or in the more concentrated 100 μg/mL GO solutions, did not exert cytotoxic effects on HGF.

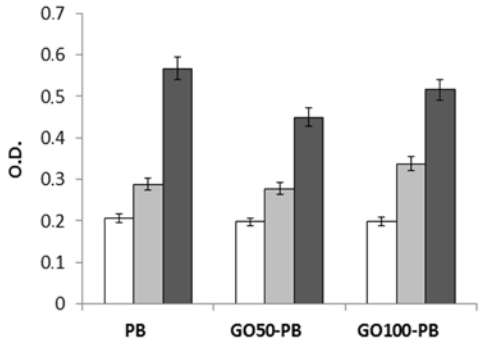

Figure 6. MTT assay in HGF seeded and cultured on PB, 50 μg/mL GO-enriched sample (GO50/PB) or 100 μg/mL GO-enriched sample (GO100/PB) for 1, 3 and 7 days. The graph represented optical density (OD) mean values (±SD) of three separate experiments. Statistical significance was evaluated through t-test. P values <0.05 were considered statistically significant.

3.7 In vivo measurements

3.7.1 Analysis of bone tissue. Following *in vitro* results, a preliminary experiment on a sheep model was undertaken to investigate *in vivo* behavior of GO-coated PB granules. In control specimens PB granules were surrounded by newly formed bone (Figure 7A). At higher magnification (40×) it was possible to see that no gaps were present at the bone-biomaterial interface and no inflammatory reaction was evident (Figure 7B). In the test specimens (i.e. GO-coated PB granules) the coating seemed to be partially detached from the particle; bone neoformation was present around both the biomaterial granules and the GO-coating (Figure 7C). At higher magnification (200×) remnants of the coating dissolved in a marrow space could be observed (Figure 7D), while no noticeable inflammatory infiltrate could be detected (Figure 7E).

The histomorphometry showed in the control samples 42.8% of newly formed bone, 19.3% of marrow spaces and 37.8% of residual biomaterial; regarding the test samples newly formed bone is 32.1%, marrow spaces are 20.2%, residual biomaterial 33.9% and graphene remnants 13.8%.

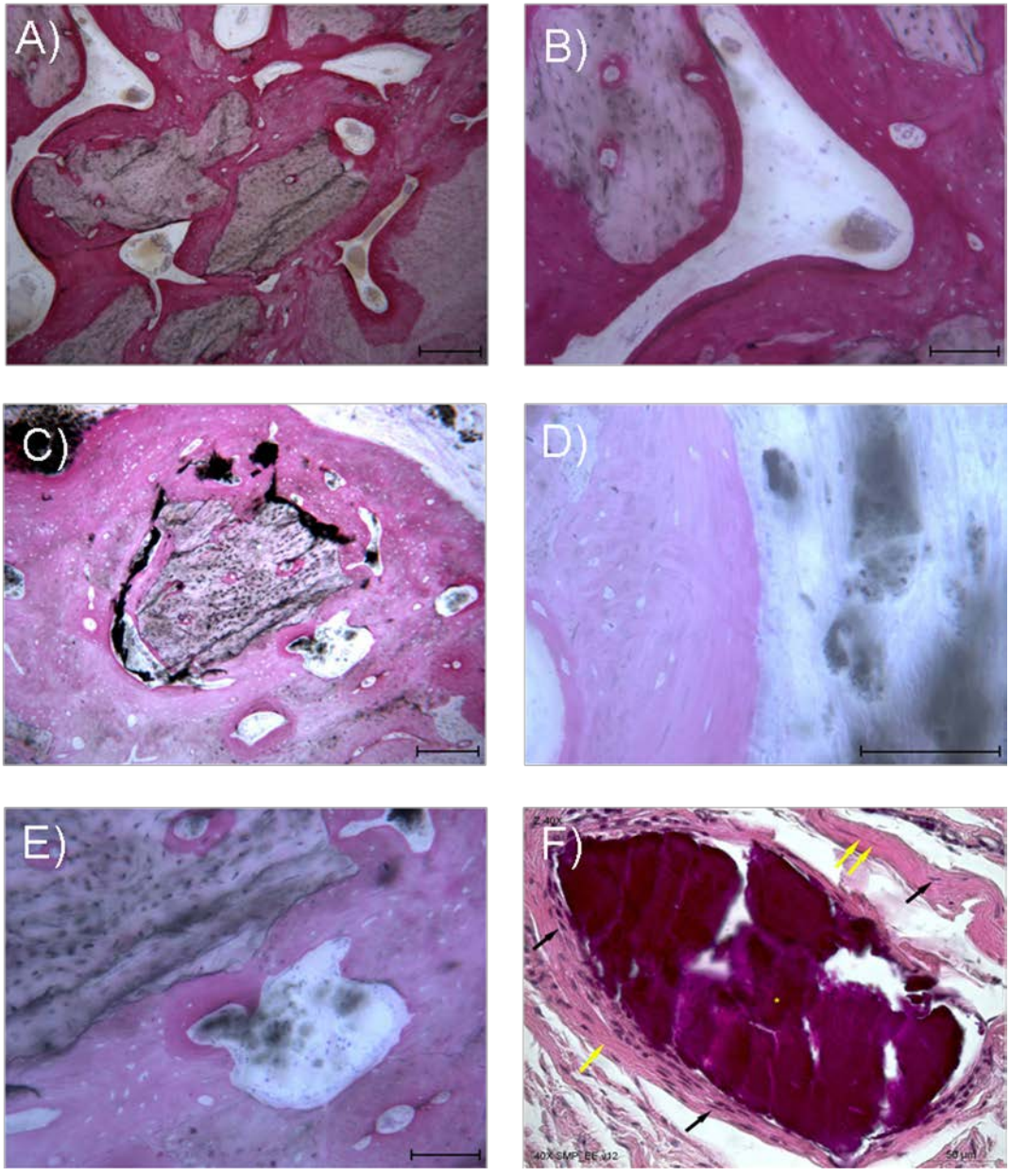

Figure 7. Light microscopy images of in vivo samples retrieved from sheep and stained with acid fuchsin-toluidine blue showing (A) PB particles surrounded by newly formed bone; (B) no gaps at the bone-biomaterial interface and no inflammatory reaction; (C) GO coating partially detached from the PB particle; (D) remnants of the GO coating dissolved in a marrow space and (E) no noticeable inflammatory infiltrate around GO/coated PB samples. A and C: magnification 40×, scale bar 200 μm. B: magnification 100×, scale bar 100 μm. D and E: magnification 200×, scale bar 100 μm. (F) Haematoxylin and eosin staining of aggregated GO visualized in the soft tissues. No inflammatory cells were present around the specimens; a defined quantity of fibroblasts as well as a significant amount of collagen fibers were observable. Scale bar: 50 μm.

3.7.2 Analysis of soft tissue and inflammatory response. Cellular response to GO-coated PB and to PB granules without GO coating are summarized in Table S2.[†] In both conditions, polymorphic nuclear cells (i.e. granulocytes), phagocytic cells (including macrophages and monocyte-derived giant cells), and non-phagocytic cells (comprising lymphocytes, plasma cells and mast cells) were absent. Images of no presence of granulocytes and macrophages in both hard and soft tissues around GO-coated PB samples (see yellow arrows in Figure 7F) were evidenced. No giant cells recruitment was observed indicating the absence of inflammatory response. A normal quantity of fibroblasts (black arrows) was present on soft tissues as well as a significant amount of collagen fibers (yellow arrows) was detected in all soft tissues confirming the good quality of tissues around the sample.

4. Discussion

The present investigation demonstrated that the synthesis of GO is straightforward and can therefore be easily scaled up at accessible costs. GO has been obtained in high yield from the almost inexpensive and easily available graphite. UV-vis, FTIR and Raman spectroscopies (see Supplementary Data) evidenced the achievement of covalently functionalized graphene, containing carbonyl, alcoholic and epoxy groups that render graphite able to solubilize in water. The highly negative ζ-potential, as compared to the literature value of -21.8±0.05 for non-functionalized pristine graphene [28], confirmed the presence of additional carboxylate groups. The dimensions of the majority of the flakes varied between 100-150 and 500-650 nm, although some micrometer flakes have been detected as demonstrated by TEM and dynamic light scattering.

The GO coating was realized by using aqueous GO solutions of different concentrations although biocompatibility and *in vivo* assays were performed on 50 μg/mL GO-coated samples. This concentration allowed to obtain ca. 1.5% GO coating easily detectable by eye (Figure 1). Raman spectroscopy evidenced the contemporary presence in the samples of hydroxyapatite and collagen (i.e. the main constituents of the heterologous bone tissue treated in order to obtain pre-formed granules) and GO. The homogeneity of the coating was checked at the micrometer scale with optical microscopy and SEM. The latter method pointed that the GO coating conferred a relatively smooth surface to the as-prepared granules. It is worth noting that the protocol used for the preparation of the hybrid material is relatively soft, therefore it is very unlikely that the observed appearance of the hybrid surface is a consequence of mechanical smoothing. This evidence is in perfect agreement

with less and smaller micro-cracks recently observed in electrochemically prepared GO-coated HA granules as compared to pure HA and indicates how GO can effectively inhibit cracks creation and propagation [29]. At the nanometer scale, TEM allowed to evidence the affinity and adhesion of GO for PB (Figure 3D). Since the investigated concentration of GO was relatively high, as testified by the fact that GO was visible by eye (see Figure 1) and a thick layer of GO covering each granule was detected by light microscopy (Figure 3A-3B), the stability and steadiness of the GO-coated PB was verified by measuring the leakage of GO in the aqueous supernatant obtained by gently shaking for 15 h a sample of GO-enriched granules. The stability results (Figure 4) evidenced that GO-coated PB granules leaked an almost negligible (less than 10% of the total amount of GO coating) amount of GO and did solubilize less calcium phosphate and collagen (Figure 4A) with respect to the naked PB granules. Indeed, positive calcium ions leaked from PB granules may draw from the GO coating negatively charged externally and weakly bound GO flakes and this in turn might favor calcium phosphates precipitation in the proximity of the granules edges. As a matter of fact, these events are in agreement with the demonstrated tendency of the carboxylate groups of GO to attract calcium ions as a strategic step for calcium phosphates deposition [30] and electrodeposition [31].

As far as mechanical features are concerned, GO showed to remarkably increase PB sample fracture resistance under compressive strain of 35%. This result is quite impressive although a 2.5 time increase of fracture toughness has been previously observed for a 2.48% enrichment with multiwalled carbon nanotubes reinforcing agent of alumina, a well known tough but brittle ceramic material [32].

The absence of any toxic leakage from GO-coated granules was confirmed by medium conditioning assays that evidenced no differences of HGF viability among naked and coated granules of both samples dipped in the cell medium used for seeding HGF cells. As far as biocompatibility analyses are concerned, no statistically significant variation of HGF viability was detected after 1, 3 and 7 days when cells were seeded directly onto immobilized granules of GO-coated PB, even when the concentration of GO was doubled to 100 μg/mL (Figure 6).

In vivo preliminary histologic observations on a sheep model evidenced bone formation around the GO-coated biomaterial particles, although aggregates of GO were observed and tended to partially dissolve in the marrow spaces and in the soft tissues (Figure 6). Nevertheless, no noticeable inflammatory infiltrate could be detected. All these evidences highlight the biocompatibility of GO-coated PB, with no evidence of inflammation both in hard and soft tissues.

Since the GO-coated PB appeared to be very stable in aqueous solutions (Figure 4) and during *in vitro* conditioning experiments for 7 days, the presence of GO aggregates in both hard and soft tissues, evidenced by preliminary *in vivo* analyses after grafting 50 μg/mL GO-coated PB granules in the animal for three months, may therefore derive from excess GO that deposited onto calcium phosphate leaked from PB granules in biological fluids and might be easily avoided by preparing a material containing a lower concentration of GO.

5. Conclusions

In the present investigation GO-coated PB granules were developed by exploiting a simple and inexpensive protocol, which could represent a model to be applied to improve the performance of other bone substitute materials. The obtained GO-coated biomaterial demonstrated to be stable over time and the strong electrostatic adhesion of GO to a hydrophilically pre-treated substrate such as PB ensured a very weak leakage of GO from the realized hybrid as evidenced by spectrophotometric, TEM and conditioning experiments. The obtained GO-coated PB granules evidenced improved mechanical features (i.e. 35%) with respect to the pure PB counterpart. The viability assays evidenced no toxic effect of GO on HGF. *In vivo* measurements did not show evidence of inflammation either in the hard or in the soft tissue. The only drawback was the leakage of aggregated GO in the soft tissue after 3 months deposition in the animal probably due to deposition of excess GO onto calcium phosphate leaked from PB granules over a 3 month period. For this reason an in-depth study will be conducted by using GO-coated samples prepared with lower concentrations of GO. The *in vivo* analysis on a larger number of animals will allow investigating the samples in terms of inflammation response and bone regeneration potential in order to tune the proper GO concentration able to exert osteoinductive properties with no toxic effects.

Funding Sources

Authors thanks POR FESR Abruzzo 2007-2013 – Activity I.1.1 Line B “Financial support for the realization of projects of industrial research and experimental development”

Supplementary Data

Materials; Apparatus and sample preparation for chemico-physical characterization; Surgery on animals; Characterization of GO; FTIR measurements; Analysis of fracture resistance and cell count.

Acknowledgement

The Authors thanks the Universities of Chieti-Pescara, Padova, Teramo and Trieste and MIUR (PRIN 2010-11, prot. 2010N3T9M4 and FIRB 2010, prot. RBAP1095CR) for financial supports.

Abbreviations

GO graphene oxide; PB porcine bone; TEM transmission electron microscopy; SEM scanning electron microscopy; HGF gingival fibroblasts; HA hydroxyapatite; CNT carbon nanotubes; DMEM Dulbecco's modified Eagle's medium; FBS fetal bovine serum; MTT 3-(4,5-dimethylthiazol-2-yl)-2,5-diphenyltetrazolium bromide; PBS buffered saline solution; v/v volume/volume DMSO dimethylsulfoxide; SD standard deviation; FTIR fourier transform infrared spectroscopy; TGA thermogravimetric analysis; UV ultraviolet; vis visible.

Notes and References

† See Supplementary Data.

[1] Lee C, Wei X, Kysar JW, Hone J. 2008, Measurement of the elastic properties and intrinsic strength of monolayer graphene, *Science*, **321**: 385–388.

[2] Balandin AA, Ghosh S, Bao W, Calizo I, Teweldebrhan D, Miao F, *et al*. 2008, Superior thermal conductivity of single-layer graphene, *Nano Lett*, **8**: 902–907.

[3] Bolotin KI, Sikes KJ, Jiang Z, Klima M, Fudenberg G, Hone J, *et al*. 2008, Ultrahigh electron mobility in suspended graphene, *Solid State Commun*, **146**: 351–355.

[4] Morozov SV, Novoselov KS, Katsnelson MI, Schedin F, Elias DC, Jaszczak JA, *et al*. 2008, Giant intrinsic carrier mobilities in graphene and its bilayer, *Phys Rev Lett*, **100**: 016602.

[5] Xia ZY, Pezzini S, Treossi E, Giambastiani G, Corticelli F, Morandi V, *et al*. 2013, The exfoliation of graphene in liquids by electrochemical, chemical, and sonication-assisted techniques: a nanoscale study, *Adv Funct Mater*, **23**: 4684–4693.

[6] Boukhvalov DW, Katsnelson MI. 2009, Chemical functionalization of graphene, *J Phys Condens Matter*, **21**: 344205.

[7] Quintana M, Montellano A, del Rio Castillo AE, Van Tendeloo G, Bittencourt C, Prato M. 2011, Selective organic functionalization of graphene bulk or graphene edges, *Chem Commun*, **47**: 9330–9332.

[8] Quintana M, Spyrou K, Grzelczak M, Browne WR, Rudolf P, Prato M. 2010, Functionalization of graphene via 1,3-dipolar cycloaddition, *ACS Nano*, **4**: 3527–3533.

[9] Bagri A, Mattevi C, Acik M, Chabal YJ, Chhowalla M, Shenoy VB. 2010, Structural evolution during the reduction of chemically derived graphene oxide, *Nat Chem*, **2**: 581–587.

[10] Yoo J, Kim J, Baek S, Park Y, Im H, Kim J. 2014, Cell reprogramming into the pluripotent state using graphene based substrates, *Biomaterials*, **35**: 8321–8329.

[11] Bressan E, Ferroni L, Gardin C, Sbricoli L, Gobbato L, Ludovichetti F, *et al*. 2014, Graphene based scaffolds effects on stem cells commitment, *J Transl Med*, **12**: 296.

[12] Doi K, Oue H, Morita K, Kajihara S, Kubo T, Koretake K, *et al*. 2012, Development of implant/interconnected porous hydroxyapatite complex as new concept graft material. *PlosOne*, **7**: e49051.

[13] Lahiri D, Ghosh S, Agarwal A. 2012, Carbon nanotube reinforced hydroxyapatite composite for orthopedic application: a review, *Mater Sci Eng C-Mater Biol Appl*, **32**: 1727–1758.

[14] Yang N, Zhang G, Li B. 2008, Carbon nanocone: a promising thermal rectifier, *Appl Phys Lett*, **93**: 243111.

[15] Kang S, Park JB, Lee TJ, Ryu S, Bhang SH, La WG, *et al.* 2015, Covalent conjugation of mechanically stiff graphene oxide flakes to three-dimensional collagen scaffolds for osteogenic differentiation of human mesenchymal stem cells, *Carbon*, **83**: 162–172.

[16] Zhao C, Lu X, Zanden C, Liu J. 2015, The promising application of graphene oxide as coating materials in orthopedic implants: preparation, characterization and cell behavior, *Biomed Mater*, **10**: 015019.

[17] Ding X, Liu H, Fan Y. 2015, Graphene-Based Materials in Regenerative Medicine, *Adv Healthc Mater*, **4**: 1451-1468.

[18] Oyefusi A, Olanipekun O, Neelgund GM, Peterson D, Stone JM, Williams E, *et al*. 2014, Hydroxyapatite grafted carbon nanotubes and graphene nanosheets: promising bone implant materials, *Spectroc Acta Pt A-Molec Biomolec Spectr*, **132**: 410–416.

[19] Liu Y, Dang Z, Wang Y, Huang J, Li H. 2014, Hydroxyapatite/graphene-nanosheet composite coatings deposited by vacuum cold spraying for biomedical applications: Inherited nanostructures and enhanced properties, *Carbon*, **67**: 250–259.

[20] Lee JH, Shin YC, Jin OS, Kang SH, Hwang Y-S, Park J-C, *et al.* 2015, Reduced graphene oxide-coated hydroxyapatite composites stimulate spontaneous osteogenic differentiation of human mesenchymal stem cells, *Nanoscale*, **7**: 11642-11651.

[21] Hummers WS, Offeman RE. 1958, Preparation of graphitic oxide, *J Am Chem Soc*, **80**: 1339–1339.

[22] Rattana T, Chaiyakun S, Witit-anun N, Nuntawong N, Chindaudom P, Oaew S, *et al.* 2012, Preparation and characterization of graphene oxide nanosheets, *Procedia Eng*, **32**: 759–764.

[23] Kolmas J, Szwaja M, Kolodziejski W. 2012, Solid-state NMR and IR characterization of commercial xenogeneic biomaterials used as bone substitutes, *J Pharm Biomed Anal*, **61**: 136–141.

[24] Li M, Wang Y, Liu Q, Li Q, Cheng Y, Zheng Y, *et al*. 2013, In situ synthesis and biocompatibility of nano hydroxyapatite on pristine and functionalized oxide, *J Mater Chem B*, **1**: 475–484.

[25] Buchwald T, Niciejewski K, Kozielski M, Szybowicz M, Siatkowski M, Krauss H. 2012, Identifying compositional and structural changes in spongy and subchondral bone from the hip joints of patients with osteoarthritis using Raman spectroscopy, *J Biomed Opt*, **17**: 017007.

[26] Hernandez Y, Nicolosi V, Lotya M, Bligh FM, Sun Z, De S, *et al.* 2008, High-yield production of graphene by liquid-phase exfoliation of graphite, *Nat Nanotechnol*, **3**: 563–568.

[27] Zappacosta R, Di Giulio M, Ettorre V, Bosco D, Hadad C, Siani G, *et al.* 2015, Liposome-induced exfoliation of graphite to few-layer graphene dispersion with antibacterial activity, just accepted for publication in *J Mater Chem B*, 3: 6520-6527.

[28] Jin Z, McNicholas TP, Shih C-J, Wang QH, Paulus GLC, Hilmer AJ, *et al*. 2011, Click chemistry on solution-dispersed graphene and monolayer CVD graphene, *Chem Mater*, **23**: 3362–3370.

[29] Li M, Liu Q, Jia Z, Xu X, Cheng Y, Zheng Y, *et al.* 2014, Graphene oxide/hydroxyapatite composite coatings fabricated by electrophoretic nanotechnology for biological applications, *Carbon*, **67**: 185–197.

[30] Kawashita M, Nakao M, Minoda M, Kim H, Beppu T, Miyamoto T, *et al*. 2003, Apatite-forming ability of carboxyl group-containing polymer gels in a simulated body fluid, *Biomaterials*, 24: 2477–2484.

[31] Zanin H, Saito E, Marciano FR, Ceragioli HJ, Granato AEC, Porcionatto M, *et al*. 2013, Fast preparation of nano-hydroxyapatite/ superhydrophilic reduced graphene oxide composites for bioactive applications, *J Mater Chem B*, **1**: 4947–4955.

[32] Lee K, Mo CB, Park SB, Hong SH. 2011, Mechanical and electrical properties of multiwalled CNT-Alumina nanocomposites prepared by a sequential two-step processing of ultrasonic spray pyrolysis and spark plasma sintering, *J. Am. Ceram. Soc*., **94**, 3774–3779.